JOURNAL OF THERMOPHYSICS AND HEAT TRANSFER
Vol. 22, No. 2, April–June 2008

Effects of Vapor Pressure on Marangoni Condensation of Steam-Ethanol Mixtures

Yusen Yang,* Junjie Yan,† Xinzhuang Wu,* and Shenhua Hu*
Xi'an Jiaotong University, 710049 Xi'an, People's Republic of China

DOI: 10.2514/1.28083

Reported herein are the experimental data for Marangoni condensation of steam–ethanol on a vertical plane surface. To clarify the effect of vapor pressure on Marangoni condensation, the heat flux and the vapor-to-surface temperature difference (surface subcooling) were measured for steam–ethanol mixtures over a wide range of compositions at vapor pressures of 84.5, 47.36, and 31.16 kPa. Seven condensation modes, smooth film, drop, film-drop, streak, drop-streak, wavy-streak, and drop with tail, were observed in this experiment. The experimental results showed that heat transfer coefficients of vapor mixtures of different compositions increased with vapor pressure. The effect of vapor pressure in enhancing the condensation heat transfer coefficient was less for pure steam and extremely high compositions (22 and 51%) than for low and middle compositions (0.5,1, 5, and 10%). The maximum heat flux and heat transfer coefficient in the condensation characteristic curves were 2.37 MW/m^2 and 0.15 MW/(m^{2}K), respectively, for a vapor velocity of 2.0 m/s, and appeared at an ethanol vapor mass fraction of approximately 1% and a pressure of 84.53 kPa. The condensation heat transfer was enhanced approximately 7.5 times compared with pure steam.

Nomenclature

A	=	area, m^2
c	=	ethanol mass fraction, %
h	=	heat transfer coefficient, kW/(m^{2}K)
M	=	mass flow rate, kg/s
M_L	=	mass flow rate of liquid, kg/s
M_V	=	mass flow rate of vapor, kg/s, $M_V = vA_{\text{sec}}\rho_V$
P	=	pressure, kPa
q	=	heat flux, kW/m^2
r	=	latent heat, kJ/kg, $r_{\text{mix}} = r_e c + r_s(1-c)$
$\bar{T}_L$	=	average temperature of liquid, K, $\bar{T}_L = (T_V + T_{\text{sur}})/2$
T	=	temperature, K
v	=	velocity of vapor, m/s
X	=	direction of heat flux
x	=	liquid mole fraction of ethanol
y	=	vapor mole fraction of ethanol
ΔT	=	surface subcooling, K
δ	=	thickness, m
λ	=	thermal conductivity, kW/(mK)
ρ	=	density, kg/m^3
σ	=	surface tension, interfacial tension, N/m

Subscripts

crest	=	crest of condensate film
e	=	ethanol
L	=	liquid
mix	=	mixture
s	=	steam
sat	=	saturated state
sec	=	cross section
sur	=	surface
V	=	vapor
valley	=	valley of condensate film
W	=	water
1, 2, 3, 4, 5	=	different layers along X direction

Superscripts

A, B, C	=	different values of pressure
a, b, c	=	different testing positions in the copper plate
av	=	average
mix	=	mixture
$'$	=	calculated results of universal quasi-chemical functional-group activity coefficients

Received 29 September 2006; revision received 27 September 2007; accepted for publication 16 October 2007.

*Graduate Research Assistant, State Key Laboratory of Multiphase Flow in Power Engineering, Department of Energy and Power.

†Professor, State Key Laboratory of Multiphase Flow in Power Engineering, Department of Energy and Power; yanjj@mail.xjtu.edu.cn.

I. Introduction

IT IS well known that the use of dropwise condensation is an effective means for heat transfer enhancement [1,2]. However, in most cases, long-term dropwise condensation is usually difficult to maintain, and so most surface condensers are designed to operate in a filmwise manner. By introducing certain amounts of more volatile heat transfer additives into the steam, a so-called Marangoni or pseudodropwise condensation on a hydrophobic surface has been observed [3–20]. In some situations, notwithstanding the vapor-phase diffusion resistance, the additive triggers interfacial turbulence that causes Marangoni convection at the vapor/liquid interface. As a result, condensation heat transfer is significantly increased.

Marangoni condensation can occur in binary mixtures which are miscible in the liquid phase and where the more volatile component has the lower surface tension. Mirkovich and Missen [3,4] first discovered this nonfilmwise condensation phenomenon and compared heat transfer coefficients of various binary vapors. It was Ford and Missen [5] who demonstrated that the criteria for film instability could be expressed simply by an inequality which was dominated by the Marangoni effect [21]. They also established a sign convention by which negative or neutral systems were stable and positive systems were unstable. Furthermore, an experimental study of condensation of ethanol-water mixtures on a horizontal tube had been studied by Fujii and Koyama [6], and five condensation modes were reported according to the prevailing conditions (composition, heat flux). An explanation of this pseudodropwise condensation was given by Hijikata et al. [7,8] who found that the condensate film is potentially unstable in these conditions. Figure 1 schematically shows a brief explanation of the Marangoni instability mechanism

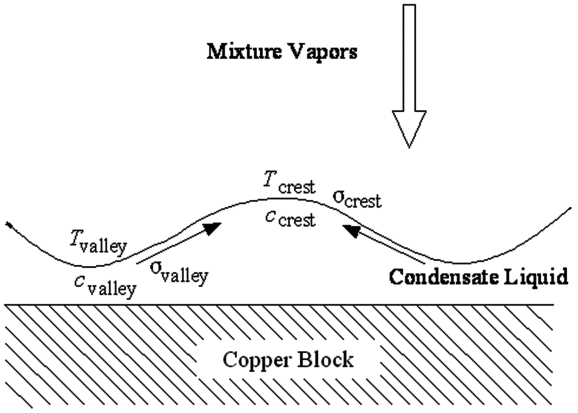

Fig. 1 Marangoni instability mechanism in condensate film.

during the Marangoni condensation process. Any turbulence in the film would be expected to give a lower film surface temperature T_{valley} where the film is thinner and a higher temperature T_{crest} at a crest ($T_{crest} < T_{valley}$). For phase equilibrium at the interface, the less volatile component (water) is then more concentrated in the liquid state at a crest than in a valley ($c_{crest} < c_{valley}$). The surface tension gradient in this case causes liquid to be drawn to the crest and the convection flow to increase ($\sigma_{crest} > \sigma_{valley}$).

The general conclusion of previous binary condensation studies [6–8] was that the heat transfer rate of binary vapor condensation was lower than that of pure vapor condensation. This lower heat transfer rate was generally attributed to there being a mass diffusion layer between the bulk vapor and the surface of the condensate film. The Marangoni effect which reduced heat transfer resistance was outweighed by the increased resistance of the diffusion layer. However, in recent years, Deans et al. [9–11], Kim et al. [12–14], and Utaka et al. [15–20] published research showing that the condensation heat transfer coefficients of mixtures with small amounts of additives were 134, 130, and 800% , respectively, that of pure steam. This meant that small amounts of additives created a significant interfacial turbulence that overcame the decrease in heat transfer caused by the diffusion resistance at the vapor/liquid interface in these circumstances. The different enhancement rates obtained by the three groups (134, 130, and 800%) come from the different concentrations of noncondensable gases, different additives, different experimental systems, and environments. According to our research [22] in 2005 and the work of Utaka et al. [15–20], noncondensable gases have great effects on the enhancement rate. The enhancement rate from our experiment [22] was 180%. But after decreasing the effects of air, the enhancement rate increased to 750% in the present data.

In a series of experiments using small vertical plane surfaces, Utaka et al. systematically studied the dependence of the vapor-side heat transfer coefficient on vapor composition (Utaka and Wang [17,19]), surface subcooling (Utaka and Terachi [16]), cross flow velocity (Utaka and Kobayashi [18]), and noncondensable gases mass fraction (Wang and Utaka [20]). Under fixed vapor composition and velocity, heat transfer coefficient was relatively low for low surface subcooling and increased steeply before decreasing again as the condensation mode shifted from dropwise to smooth film as subcooling temperature increased. The effect of velocity was to augment the heat transfer coefficient due to reduction in the diffusion resistance, as well as to the shear stress effect on the condensate surface. Under optimum conditions of low ethanol composition and high vapor velocity, the condensation heat transfer was enhanced approximately 2–8 times as compared with that of pure steam. However, the peak heat transfer coefficient decreased greatly with increased concentration of the noncondensable gases. In particular, the decrease was greatest at low ethanol composition and low noncondensable gases concentration.

The preceding experiments were all performed at either atmospheric pressure or a single vapor pressure. However, because detailed research concerning the effect of vapor pressure on Marangoni condensation has not yet been reported, the objective of the present study is to clarify the effect of vapor pressure on nonfilmwise condensation of a steam–ethanol mixture.

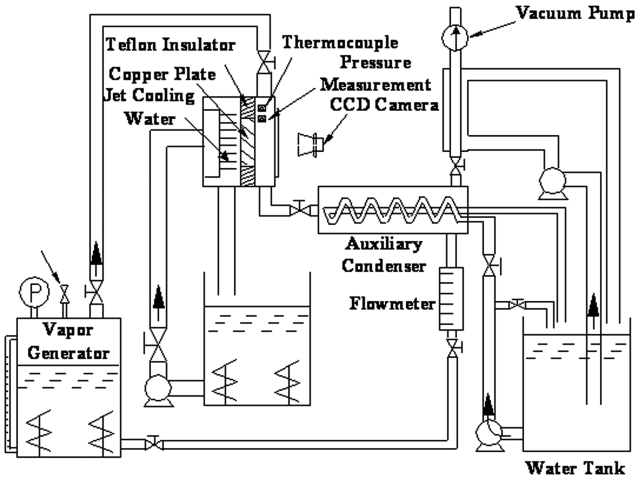

Fig. 2 Diagram of the experimental apparatus.

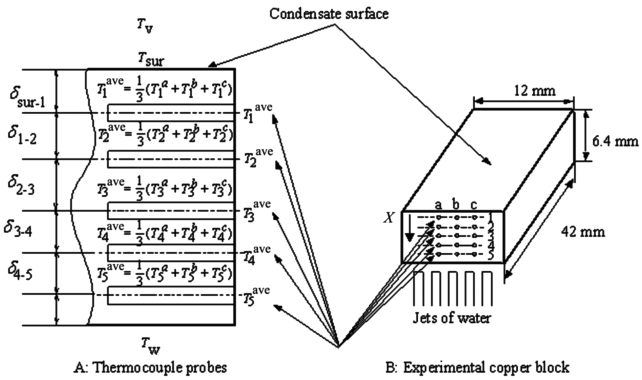

Fig. 3 Schematic of the measurement system for the copper plate.

II. Experimental Apparatus

The experimental apparatus is shown schematically in Fig. 2. It was composed of a closed natural circulation loop containing the steam–ethanol mixture and a second circuit containing the water coolant. For the binary mixture natural circulation loop, the mixture was vaporized using an electrically heated boiler (maximum power 10 kW). The vapor mixture was let into the upper entrance of a vertically oriented rectangular cross-section duct, where it condensed on the vertical surface of a copper plate. The remaining vapor was liquefied completely in an auxiliary condenser. For the second circuit, the jet cooling water was heated electrically in a tank and circulated by a pump. The condensation pressure in the condensing chamber was measured by a pressure transducer. Using the mixture mass flow rate measured by a calibrated flowmeter, the cross-sectional area, and the condensation pressure, the vapor velocity through the condensate surface was calculated. The vacuum pump and the cooling water system worked throughout the experiment to avoid the influence of noncondensable gases. The prescribed pressure in the condensing chamber was obtained by adjusting the cooling water valve on the condenser.

III. Method of Measurement

A. Measurement of Heat Transfer Coefficient

Figure 3 shows the temperature measurement system for the copper plate. The condensate surface had an area of 12×42 mm. Two assumptions were made in the calculations: 1) One-dimensional conduction heat transfer along the X direction was assumed, because

the copper plate was insulated from the surroundings using a thick Teflon plate, i.e., heat loss in other directions could be neglected. 2) The thermal conductivity of the copper plate was constant in each region of thickness δ which depended on the average temperature $T_1^{av} \sim T_5^{av}$, respectively. The relationship between the thermal conductivity of the copper and temperature could be obtained by polynomial regression.

According to the preceding assumptions, the heat transfer coefficient was determined as follows:

$$h = \frac{q}{T_V - T_{sur}} \tag{1}$$

and

$$q = -\lambda(T)\frac{dT}{dX} \tag{2}$$

where the heat flux q is obtained by averaging the heat flux values through the copper plate

$$q = \frac{1}{4}\left[\lambda\frac{T_1^{av} - T_2^{av}}{\delta_{1-2}} + \lambda\frac{T_2^{av} - T_3^{av}}{\delta_{2-3}} + \lambda\frac{T_3^{av} - T_4^{av}}{\delta_{3-4}} + \lambda\frac{T_4^{av} - T_5^{av}}{\delta_{4-5}}\right] \tag{3}$$

The mean temperature of the condensate surface T_{sur} is calculated by extrapolating the temperature profile from the copper plate:

$$T_{sur} = T_1^{av} + \frac{q}{\lambda}\delta_{sur-1} \tag{4}$$

Thus, to obtain q or h, the measurement of the following 16 temperatures, T_V, $T_1^a \sim T_5^a$, $T_1^b \sim T_5^b$, $T_1^c \sim T_5^c$, and four distances, δ_{1-2}, δ_{2-3}, δ_{3-4}, δ_{4-5}, is needed. The temperature in the copper plate was measured by inserting 15 0.2 mm T-type thermocouple probes (copper vs copper–nickel, Omega, calibrated before all experiments), and the vapor temperature and the cooling water temperature were also measured by this type of thermocouple.

B. Measurement of Vapor Composition

The generated vapor composition during the boiling process was found to coincide with the composition given by the vapor–liquid phase equilibrium relation and to be independent of the boiling conditions. Therefore, the vapor composition was obtained by vapor–liquid phase equilibrium relations.

The UNIFAC [universal quasi-chemical (UNIQUAC) functional-group activity coefficients] method was used to determine the vapor composition of the vapor mixture. The UNIFAC model performed well for most higher polar compounds, e.g., ethanol and water mixtures [23], and was derived from the UNIQUAC model by Fredenlund et al. [24] in 1975. Based on this model, a program was developed to calculate the vapor composition using the liquid composition under different vapor pressures. Under a vapor pressure of 6.7 kPa, the computational results of UNIFAC were compared with the experimental data of [25] in Table 1, and they agree within 9.1% error. This indicated that the UNIFAC program was reliable.

Table 1 Comparison of experimental data in [25] and computational results of UNIFAC

Liquid composition	Experimental data in [25]		Results of UNIFAC	
x	y	T	y'	T'
mol%	mol%	°C	mol%	°C
8.6	40.80	29.40	44.53	28.99
11.1	46.80	28.15	48.18	28.07
14.2	51.20	27.10	51.37	27.26
37.9	63.20	23.90	63.18	24.56
47.8	66.90	23.25	67.18	23.90
78.0	82.20	21.95	82.28	22.48
88.5	89.80	21.70	89.46	22.24

C. Measurement of Vapor Pressure

The steam pressure was measured by a pressure transducer (Measurement Specialties, Inc., accuracy 0.1%), for which the pressure tap was located on the duct wall beside the condensate surface, as shown in Fig. 2. The vapor pressure was varied by adjusting the cooling water valve on the condenser, and the experiments were carried out at three prescribed pressures which were 31.16, 47.36, and 84.53 kPa.

D. Measurement of Noncondensable Gases

Because the present data were obtained below atmospheric pressure, the presence of air in the vapor cannot be ignored, according to the paper of Wang and Utaka [20]. First, the vapor system was tested for any leaks to minimize the detrimental effect of noncondensable gases on the condensation process. The apparatus was evacuated for about 20 min to reach a minimum pressure of 1000 Pa, then the vacuum pump was stopped. The pressure increased 350 Pa over 24 h without heating, and the amount of air present in the system was calculated to be approximately 50 ppm, a level that ensured the experimental results would be reliable and usable [20].

E. Uncertainty Analysis

The experimental data reduction scheme relied on accurate test measurements. The uncertainties were associated with raw measurements and the derived data that were analyzed using the method of Moffat [26]. The uncertainty in the thermal conductivity λ was 2%, in T was 0.1°C, in δ was 2×10^{-5} m, and that of the noncondensable air mass fraction was 6 ppm. The uncertainties of q and h were $4 \sim 18\%$ and $4 \sim 19\%$, respectively.

IV. Experimental Results and Discussion

A. Observation of the Condensation Mode

In the experimental studies by our group or others, the condensate modes were determined by the vapor composition, vapor velocity, surface subcooling, and vapor pressure. Seven condensation modes, smooth film, drop, film-drop, streak, drop-streak, wavy-streak, and drop with tail, were observed in our experiment. The photographs are shown in Fig. 4. The condensation mode of pure steam or pure ethanol was smooth film condensation. However, vapor mixtures with compositions of 0.5–51% were mostly nonfilmwise condensation. With a decrease in surface subcooling during each experimental test, the condensation mode changed from smooth film to drop, then to drop-streak, to wavy-streak or streak, and finally to smooth film.

Figure 5 shows the different condensation modes and different characteristic curves under two vapor pressures, two vapor compositions, and three surface subcooling conditions. This illustrates that, under the maximum surface subcooling, the condensation mode for low ethanol composition (2%) was commonly drop-film, as shown in pictures a1 and a2 of Fig. 5, whereas that for high ethanol composition (51%) was filmwise, as shown in pictures a3 and a4 of Fig. 5. As the heat transfer coefficient reached its maximum value, drops appeared on the condensation surface under low and high ethanol compositions. The drops were big and sparse under low pressure, as given in pictures b2 and b4 of Fig. 5, and small and dense under high pressure, shown in pictures b1 and b3 of Fig. 5. When the surface subcooling was about 5 K, the condensate characteristics for high ethanol composition (51%) was pure filmwise, but for low ethanol composition (2%), it was the streak mode; the streaks were thick and sparse under low pressure, as shown in picture c2 of Fig. 5, but thin and dense under high pressure as shown in picture c1 of Fig. 5. In addition, under low vapor pressure, the observed diameters of departing drops were bigger, the sweeping frequency was lower, and the mass flow rate of total condensate was smaller; whereas, for the high vapor pressure, the diameters were smaller, the frequency was higher, and the mass flow rate was larger.

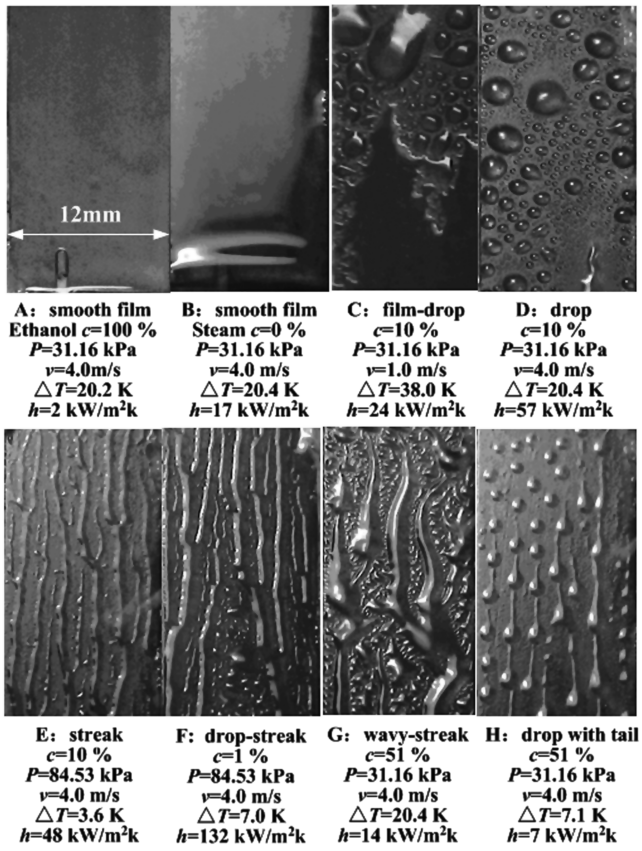

Fig. 4 Different condensation modes for pure vapors and vapor mixtures.

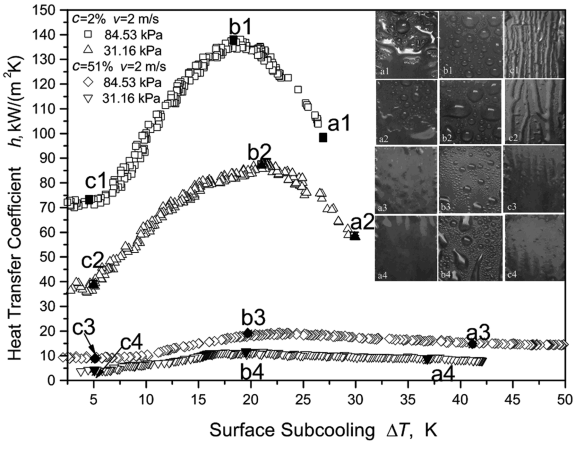

Fig. 5 Condensation modes and characteristic curves under different pressures, compositions, and temperature differences.

B. Experimental Results of Pure Steam and the Predictions from Nusselt's Theory

For pure steam condensation, after more than a hundred hours of commissioning tests, the condensate surface changed naturally to a wetting surface. The initial dropwise condensation shifted to a smooth film. This natural method of obtaining smooth film condensation of pure steam was different from the method in Utaka and Wang's experiment [19]. Utaka and Wang applied oxidized titanium to the condensate surface to achieve a wetting surface and smooth film condensation for pure steam. Hence, the condensation mode for pure steam was filmwise by both groups, and the predictions of Nusselt's theory [27] could be applied. Figure 6 shows that the experimental results of steam agreed well with the predictions of Nusselt's theory, indicating that the measurement system and experimental method were reliable.

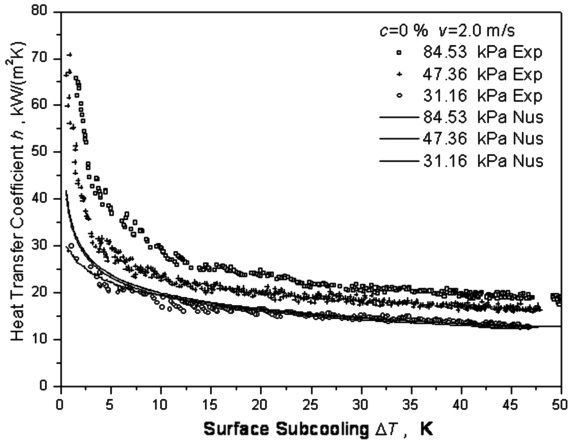

Fig. 6 Comparison of experimental results and Nusselt analysis.

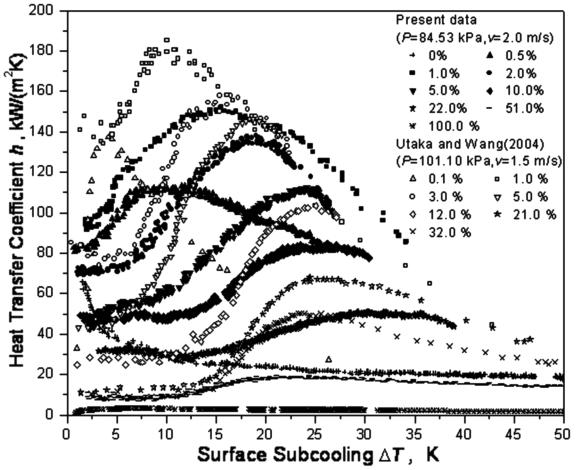

Fig. 7 Comparison of present condensation characteristics curves with those of Utaka and Wang [19] for various percentages of ethanol c.

C. Effect of Vapor Composition and Surface Subcooling

All tests were carried out at an approach velocity of $v = 2.0$ m/s, and the inlet vapor ethanol composition was varied from 0.5 to 51%. The experimental results from separate days but under the same conditions showed good repeatability. Figure 7 shows the influences of composition and surface subcooling on heat transfer coefficients at the same vapor pressure of $P = 84.53$ kPa and the same vapor velocity of $v = 2.0$ m/s. The experimental results of Utaka and Wang [19] under a vapor pressure of $P = 101.1$ kPa and an approach vapor velocity of $v = 1.5$ m/s are also shown in Fig. 7.

Our data and that of Utaka and Wang [19] showed similar trends when the effects of vapor composition and surface subcooling were considered. These similar trends are summarized as follows:

1) The dependence of heat transfer on surface subcooling and mass fraction was evidently related to changes in the condensation mode. This was proven by the observations made.

2) Heat transfer coefficient varied when ethanol mass fraction changed. When ethanol mass fraction was 1%, heat transfer coefficient reached its maximum value for the present data of 150 kW/(m^{2}K), and for the data of Utaka and Wang [19] of 188 kW/(m^{2}K).

3) When the vapor composition was lower than 22%, heat transfer coefficients of vapor mixtures were higher than those of steam, but when the composition was 51%, heat transfer coefficients were lower than those of steam. The heat transfer coefficient of pure ethanol was lowest at all compositions.

4) For a fixed vapor composition, the relationship between heat transfer coefficient and surface subcooling revealed a remarkably nonlinear nature. The heat transfer coefficient of the vapor mixture

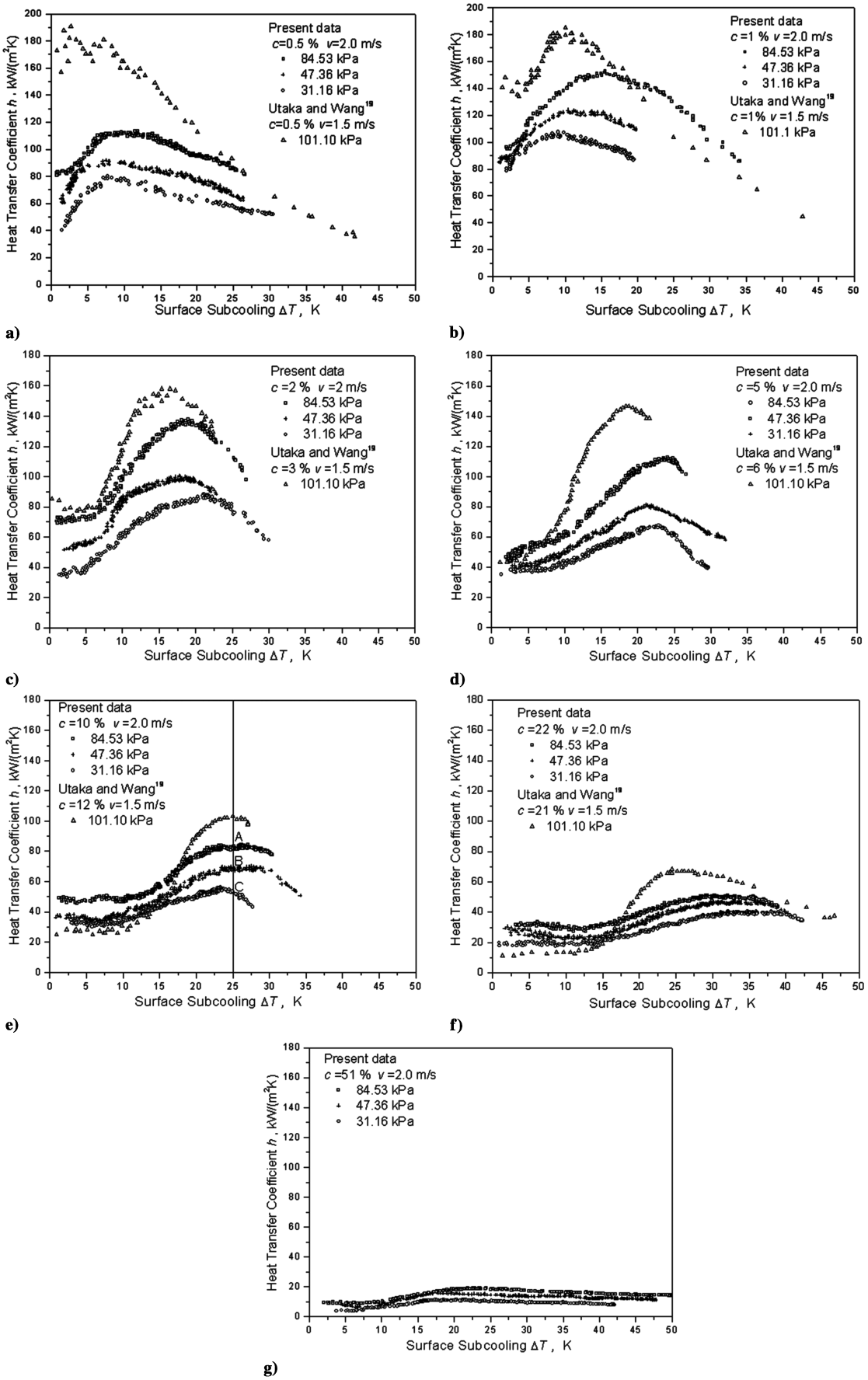

Fig. 8 Condensation characteristic curve for Marangoni condensation under different pressures: a) $c = 0.5\%$, b) $c = 1\%$, c) $c = 2\%$, d) $c = 5\%$, e) $c = 10\%$, f) $c = 22\%$, g) $c = 51\%$.

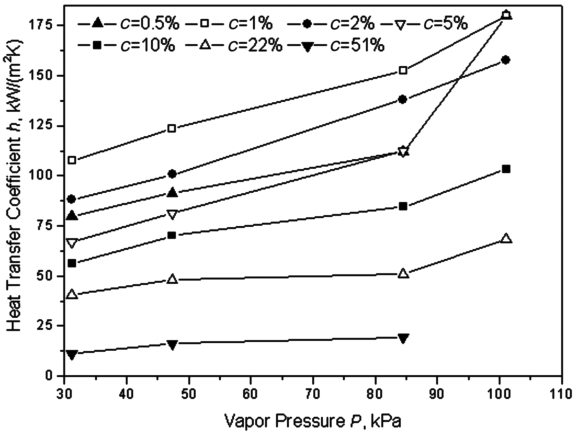

Fig. 9 Maximum heat transfer coefficient vs pressure under different percentages of ethanol *c*.

was comparatively low when surface subcooling was lower than about 10 K. In this range of subcooling temperatures, the diffusion resistance of the vapor phase was large. Then, as surface subcooling rose, heat transfer coefficient increased linearly and steeply to a maximum point, due to the dropwise mode of the condensate and the reduction of diffusion resistance. With further increase in subcooling temperature, heat transfer coefficient decreased with a transition of the condensation mode from dropwise to filmwise.

However, there were two differences between the present data and the data of Utaka and Wang [19]. First, the peak value of heat transfer coefficient in the work of Utaka and Wang [19] was higher than that of the present data. This was attributed to the effect of vapor pressure and noncondensable gases (because the present data was obtained under subatmospheric pressure conditions, whereas that of Utaka and Wang came from atmospheric pressure conditions). Second, in the domain controlled by diffusion resistance ($\Delta T < 10$ K), heat transfer coefficients of the present data were higher than those of Utaka and Wang [19]. This difference resulted from the different methods of obtaining the filmwise condensation as discussed in Sec. IV.B.

D. Effect of Vapor Pressure

Figure 8 plots heat transfer coefficient vs surface subcooling calculated by Eq. (1) for the present results and for those of Utaka and Wang [19] under similar conditions (c and v). Separate graphs were plotted for different experimental conditions. The different symbols in each graph represent different vapor pressures. The results in Fig. 8 demonstrate that heat transfer coefficient increases with vapor pressure. It may also be seen that heat transfer coefficients of mixtures with higher compositions of 22 and 51% increased slightly with vapor pressures, but for mixtures with low and middle compositions of 0.5, 1, 5, and 10%, heat transfer coefficients rose strongly. When surface subcooling was 20 K, the coefficients of the vapor mixtures increased with pressure as shown in Fig. 9.

For $c = 9.8\%$, $\Delta T = 25$ K, and $v = 2.0$ m/s, the heat transfer coefficient for three prescribed pressures A, B, and C is plotted in Fig. 8e. The values of pressures for A, B, and C are given in Table 2. By the comparison of these results for different vapor pressures, the reasons for different heat transfer performance at the three pressures are given as follows:

1) As vapor pressure rose, vapor density increased rapidly and induced an increase in vapor mixture mass velocity M_V as shown in Table 2. In the microscopic view, vapor molecules gathered densely at high vapor pressure, but at low vapor pressures, the density was lower, and the molecules passed the surface in low concentrations.

2) Under the same surface subcooling, heat flux for high vapor pressure was larger than that for low vapor pressure. However, the latent heat r for high pressure was smaller than that for low pressure. Thus, the mass flow rate of condensate liquids M_L at high pressure was larger than that at low pressure.

3) The average temperature of the condensate $\bar{T}_L$ was another remarkable difference among pressures A, B, and C. The relationship was

$$\overline{T_L^A} > \overline{T_L^B} > \overline{T_L^C} \tag{7}$$

The binary mixtures of steam–ethanol were "positive systems" [3], i.e., the surface tension, composition, and temperature had following relationships:

$$\left(\frac{\partial\sigma}{\partial T}\right)_{\text{sat}} \equiv \left(\frac{\partial\sigma}{\partial c}\right)_{\text{sat}}\left(\frac{\partial c}{\partial T}\right)_{\text{sat}} \tag{8}$$

$$\left(\frac{\partial\sigma}{\partial c}\right)_{\text{sat}} < 0 \tag{9}$$

$$\left(\frac{\partial c}{\partial T}\right)_{\text{sat}} < 0 \tag{10}$$

$$\left(\frac{\partial\sigma}{\partial T}\right)_{\text{sat}} > 0 \tag{11}$$

Equation (10) shows that the higher the temperature, the lower the composition of the condensate. Equation (9) indicates that the lower the composition, the higher the surface tension for high-pressure conditions. On the other hand, Eq. (11) shows that surface tension increases with temperature, but according to Vemuri et al. [13], the temperature dependency of surface tension in this case ($\partial\sigma/\partial T$) is secondary. Based on Eqs. (7–11), we find the following simple inequality:

$$\sigma^{\text{A}} > \sigma^{\text{B}} > \sigma^{\text{C}} \tag{12}$$

Equation (12) shows that the surface tension of condensate increases with vapor pressure when other experimental conditions are fixed.

Based on the three reasons given previously, when the pressure rose, the increases in M_V, M_L, and σ induced an increased disturbance in the condensate film and the vapor–liquid interface.

Table 2 Comparison of parameters for three pressures

Parameters	Units	A, $P = 84.53$ kPa	B, $P = 47.36$ kPa	C, $P = 31.16$ kPa
ΔT	°C	25.00	25.00	25.00
h	kW/(m^{2}K)	82	69	53
q	kW/m^2	2043	1732	1327
$\bar{T}_L$	°C	82.5	67.5	57.5
ρ_v^{mix}	kg/m^3	0.59	0.34	0.23
r_{mix}	kJ/kg	2118	2155	2179
A_{sec}	m^2	1.30×10^{-3}	1.30×10^{-3}	1.30×10^{-3}
A_{sur}	m^2	5.04×10^{-4}	5.04×10^{-4}	5.04×10^{-4}
M_V	kg/s	1.5×10^{-3}	0.9×10^{-3}	0.6×10^{-3}
M_L	kg/s	4.9×10^{-4}	4.1×10^{-4}	3.1×10^{-4}

This disturbance caused an enhancement in the heat transfer coefficient.

V. Conclusions

In this paper, new experimental data were presented for Marangoni condensation under different vapor pressures. It was found that the effect of vapor pressure in enhancing the condensation heat transfer coefficient was significantly greater for mixtures with low and middle compositions of 0.5, 1, 2, 5, and 10%, than for mixtures with high compositions of 22 and 51%. When the present results were compared with the earlier data of Utaka and Wang [19], condensation characteristic curves were similar, indicating that significant heat transfer enhancement may be obtained through the addition of very small amounts of ethanol to boiler feed water. Differences between the present results and those of Utaka and Wang [19] were caused by the effects of vapor pressure and noncondensable gases, or the different methods of obtaining filmwise condensation, as discussed in Sec. IV.B. The mechanism for Marangoni condensation is understood in general, but the method for modeling this process requires further investigation.

Acknowledgment

This project has been supported by National Natural Science Foundation of China through grant numbers 50476048 and 50521604.

References

[1] Collier, J. G., *Convective Boiling and Condensation*, 2nd ed., McGraw–Hill, New York, 1981, Chaps. 8, 12.

[2] Kakac, S., and Liu, H., *Heat Exchangers*, CRC Press, Boca Raton, FL, 1998, Chaps. 6, 7.

[3] Mirkovich, V. V., and Missen, R. W., "Non-Filmwise Condensation of Binary Vapors of Miscible Liquids," *Canadian Journal of Chemical Engineering*, Vol. 39, No. 4, 1961, pp. 86–87.

[4] Mirkovich, V. V., and Missen, R. W., "Study of the Condensation of Binary Vapors of Miscible Liquids, Part 2: Heat Transfer Coefficients for Filmwise and Non-Filmwise Condensation," *Canadian Journal of Chemical Engineering*, Vol. 41, No. 4, 1963, pp. 73–78.

[5] Ford, J. D., and Missen, R. W., "On the Conditions for Stability of Falling Films Subject to Surface Tension Disturbances: The Condensation of Binary Vapors," *Canadian Journal of Chemical Engineering*, Vol. 48, No. 10, 1968, pp. 309–312.

[6] Fujii, T., and Koyama, S., "Gravity Controlled Condensation of an Ethanol and Water Mixture on a Horizontal Tube," *Transactions of the Japan Society of Mechanical Engineers, Series B*, Vol. 55, No. 1, 1989, pp. 210–217.

[7] Hijikata, K., Fukasaku, Y., and Nakabeppu, O., "Instability Analysis of the Drop Growth Mechanism on Condensation of a Water-Ethanol Binary Mixture," *Transactions of the Japan Society of Mechanical Engineers, Series B*, Vol. 60, No. 572, 1994, pp. 1337–1342.

[8] Hijikata, K., Fukasaku, Y., and Nakabeppu, O., "Theoretical and Experimental Studies on the Pseudo-Dropwise Condensation of a Binary Vapor Mixture," *Journal of Heat Transfer*, Vol. 118, Feb. 1996, pp. 140–147.

[9] Morrison, J. N. A., Philpott, C., and Deans, J., "Augmentation of Steam Condensation Heat Transfer by Addition of Methylamine," *International Journal of Heat and Mass Transfer*, Vol. 41, No. 22, 1998, pp. 3679–3683. doi:10.1016/S0017-9310(97)00345-1

[10] Morrison, J. N. A., and Deans, J., "Augmentation of Steam Condensation Heat Transfer by Addition of Ammonia," *International Journal of Heat and Mass Transfer*, Vol. 40, No. 4, 1997, pp. 765–772. doi:10.1016/0017-9310(96)00178-0

[11] Philpott, C., and Deans, J., "Condensation of Ammonia-Water Mixtures in a Horizontal Shell and Tube Condenser," *Journal of Heat Transfer*, Vol. 126, No. 4, 2004, pp. 527–534. doi:10.1115/1.1778188

[12] Kim, K. J., Lefsaker, A. M., Razani, A., and Stone, A., "Effective Use of Heat Transfer Additives for Steam Condensation," *Applied Thermal Engineering*, Vol. 21, No. 18, 2001, pp. 1863–1874. doi:10.1016/S1359-4311(01)00059-X

[13] Vemuri, S., Kim, K. J., Razani, A., Bell, T. W., and Wood, B. D., "Cost-Effective Techniques for Enhancing Heat Transfer Rate in Steam Condensation," *Journal of Thermophysics and Heat Transfer*, Vol. 19, No. 1, 2005, pp. 101–105.

[14] Vemuri, S., and Kim, K. J., "An Experimental and Theoretical Study on the Concept of Dropwise Condensation," *International Journal of Heat and Mass Transfer*, Vol. 49, Nos. 3–4, 2006, pp. 649–657. doi:10.1016/j.ijheatmasstransfer.2005.08.016

[15] Utaka, Y., and Terachi, N., "Study on Condensation Heat Transfer for Steam-Ethanol Vapor Mixture (Relation Between Condensation Characteristic Curve and Modes of Condensate)," *Transactions of the Japan Society of Mechanical Engineers, Series B*, Vol. 61, No. 588, 1995, pp. 3059–3065.

[16] Utaka, Y., and Terachi, N., "Measurement of Condensation Characteristic Curves for Binary Mixture of Steam and Ethanol Vapor," *Heat Transfer, Japanese Research*, Vol. 24, No. 1, 1995, pp. 57–67.

[17] Utaka, Y., and Wang, S., "Promotion of Steam Condensation Heat Transfer Using Solutal Marangoni Condensation," *Transactions of the Japan Society of Mechanical Engineers, Series B*, Vol. 68, No. 1, 2002, pp. 148–156.

[18] Utaka, Y., and Kobayashi, H., "On Condensation Heat Transfer for Water and Ethanol Vapor Mixture (Characteristics over a Wide Range of Vapor Velocity)," *Transactions of the Japan Society of Mechanical Engineers, Series B*, Vol. 67, No. 1, 2001, pp. 141–147.

[19] Utaka, Y., and Wang, S., "Characteristic Curves and the Promotion Effect of Ethanol Addition on Steam Condensation Heat Transfer," *International Journal of Heat and Mass Transfer*, Vol. 47, No. 21, 2004, pp. 4507–4516. doi:10.1016/j.ijheatmasstransfer.2003.07.032

[20] Wang, S., and Utaka, Y., "An Effect of Non-Condensable Gas Mass Fraction on Condensation Heat Transfer for Steam-eEthanol Vapor Mixture," *Japan Society of Mechanical Engineers International Journal, Series B*, Vol. 47, No. 2, 2004, pp. 162–167.

[21] Scriven, L. E., and Sternling, C. V., "Marangoni Effects," *Nature (London)*, Vol. 187, No. 4733, 1960, pp. 186–188. doi:10.1038/187186a0

[22] Yan, J., Yang, Y., Hu, S., Zhen, K., and Liu, J., "Effects of Vapor Pressure/Velocity and Concentration on Condensation Heat Transfer for Steam–Ethanol Vapor Mixture," *Heat and Mass Transfer*, Vol. 44, No. 1, 2007, pp. 51–60. doi:10.1007/s00231-006-0216-5

[23] Claudio, A. F., and Valderrama, J. O., "Phase Equilibrium Modeling in Binary Mixtures Found in Wine and Must Distillation," *Journal of Food Engineering*, Vol. 65, No. 6, 2004, pp. 577–583.

[24] Fredenlund, A., Jones, R. L., and Prausnitz, J. M., "Group Contribution Estimation of Activity Coefficients in Non-Ideal Liquid Mixtures," *American Institute of Chemical Engineers Journal*, Vol. 21, No. 6, 1975, pp. 1086–1099. doi:10.1002/aic.690210607

[25] Gmehling, J., *Vapor-Liquid Equilibrium Data Collection: Organic Hydroxy Compounds: Alcohol and Phenols, Chemistry Data, Series 1*, Dechema, Frankfurt, 1978, Pt. 2a.

[26] Moffat, R. J., "Contributions to the Theory of Single-Sample Uncertainty Analysis," *Journal of Fluids Engineering*, Vol. 104, No. 2, 1982, pp. 250–260.

[27] Tanasawa, I., "Advances in Condensation Heat Transfer," *Advances in Heat Transfer*, Vol. 21, 1991, pp. 55–139.